This is a preprint of: "Dynamics of the secand map near infinity", Antoni Garijo, Xavier Jarque, *J. Difference Equ. Appl.*, vol. 28(10), 1334–1347, 2023.
DOI: [10.1080/10236198.2022.2044476]

DYNAMICS OF THE SECANT MAP NEAR INFINITY

ANTONIO GARIJO AND XAVIER JARQUE

Abstract. We investigate the root finding algorithm given by the secant method applied to a real polynomial p as a discrete dynamical system defined on $\mathbb{R}^2$. We extend the secant map to the real projective plane $\mathbb{RP}^2$, proving the existence of an attracting fixed point on the line of infinity, which allow us to better understand the dynamics of the secant method near ∞. Moreover, this fixed point only depends on the degree of the polynomial p.

Keywords: Root finding algorithms, iteration, secant method.

1. Introduction and preliminaries

Root finding algorithms are not only an efficient way to find numerical solutions of non linear equations which cannot be solve explicitly but a fruitful source of interesting dynamical systems. The common idea behind any such algorithm is to construct sequences converging to the solutions of the equation, and these sequences correspond to orbits of discrete dynamical systems.

Let X be a topological space. Roughly speaking a discrete dynamical system over X (known as *phase space*) is a map $f : X \to X$ and the orbits induced by this map starting at $x_0 \in X$, $\{x_n := f^n(x_0)\}_{n\in\mathbb{N}}$. The main goal is to describe the *phase portrait*, that is the description of the asymptotic behaviour of those orbits when x_0 runs over all X. We say that ζ in X is a fixed point if $f(\zeta) = \zeta$. We say that ζ is attracting or repelling depending if all nearby seeds correspond to orbits converging or divergingto ζ. It is well known that fixed (as well as periodic) points play a key role to understand the global dynamics, specially when f models a root finding algorithm. In the case that ζ in X is an attracting fixed point we define its *basin of attraction* by

$$A(\zeta) = \{x \in X \mid f^n(x) \to \zeta, \text{ as } n \to \infty\},$$

or, in other words, $A(\zeta)$ is the maximal set where orbits converge to ζ under iteration. The connected component of $A(\zeta)$ which contains x_0 is called the *immediate basin of attraction of* ζ and it is denoted by $A^\star(\zeta)$.

Why discrete dynamical systems are related with root finding algorithms is almost direct. Suppose we want to solve the nonlinear equation $p(x) = 0$. A root finding algorithm can be understood as a discrete dynamical system $f_p : X \to X$ so that its orbits $\{x_n := f_p^n(x_0)\}_{n\in\mathbb{N}}$, converge to the solutions of $p(x) = 0$ for *most* initial conditions $x_0 \in X$. For instance, studing the global phase portrait associated to f_p gives valuable information on how to choose the initial conditions to find *all* solutions of $p(x) = 0$ (see [HSS01] for the case that p is a polynomial with complex coefficients).

To simplify the exposition we focus on the case that the nonlinear equation $p = 0$ is given by a polynomial with complex coefficients. The most well-known and universal root finding

Date: January 20, 2022.
This work has been partially supported by MINECO-AEI grants PID2020-118281GB-C32 and PID2020-118281GB-C33, and the AGAUR grant 2017SGR1374.

algorithm to find out the roots of p is *Newton's method* defined as the iterates of the Newton's map

$$N := N_p(z) = z - \frac{p(z)}{p'(z)}. \tag{1}$$

Observe that $p(\alpha) = 0$ if and only if $N_p(\alpha) = \alpha$. Moreover, easy computations show that $|N_p'(\alpha)| < 1$ and so the roots of p are attracting fixed points of N_p, in fact if α is a simple root then $N_p'(\alpha) = 0$, and one of the major interest is to study the basins of attraction of the different roots of p as well as their boundaries which are contained in the Julia set of N_p.

A first step is to extend the Newton map to the point at infinity, that is, to extend the phase space from $\mathbb{C}$ to $\hat{\mathbb{C}} = \mathbb{C} \cup \{\infty\}$, where $\hat{\mathbb{C}}$ denotes the Riemann sphere. Using appropriate charts on $\hat{\mathbb{C}}$ we can see that $z = \infty$ is always a repelling fixed point of N_p.

It is worth to be noticed that Newton's method was the starting point of holomorphic dynamics when Cayley used dynamical systems to understand the phase portrait of Newton's method applied to low degree polynomials (see [Cay79a, Cay79b, Cay80]). Because of the importance of this universal root finding algorithm there is a wide literature on different aspects of Newton's method, including recent results for the non polynomial case. See for instance [HSS01, Shi09, BFJK14, BFJK18]).

An alternative to Newton's method is the *Secant's method*. Although it admits a complex variable version (see [BF19] and Section 4 in this paper) in this work we focus on the (real) Secant's method applied to real polynomials of the form

$$p(x) = a_k x^k + \ldots + a_1 x + a_0, \ a_k \neq 0, \tag{2}$$

with $k \geq 3$. We also assume that p has n real simple roots $\alpha_0 < \alpha_1 < \ldots < \alpha_{n-1}$ with $n \in \{0, \ldots, k\}$. The roots α_0 and α_{n-1} are called *external* roots and the rest *internal* roots. The secant's method is the root finding algorithm defined as the iterates of the Secant's map $S := S_p : \mathbb{R}^2 \mapsto \mathbb{R}^2$ given by

$$S : \begin{pmatrix} x \\ y \end{pmatrix} \mapsto \begin{pmatrix} S_1(x,y) \\ S_2(x,y) \end{pmatrix} = \begin{pmatrix} y \\ y - p(y)\frac{y-x}{p(y)-p(x)} \end{pmatrix} = \begin{pmatrix} y \\ \frac{yp(x)-p(y)x}{p(x)-p(y)} \end{pmatrix}. \tag{3}$$

Observe that in contrast to Newton's method, the phase space of the Secant's method is two dimensional: $\mathbb{R}^2$ or $\mathbb{C}^2$ in its complex version. To visualize this, consider the Chebychev's polynomial $p_4(x) = 1 - 8x^2 + 8x^4$ having all four single roots in the interval $(-1, 1)$. So, given a root $z = \alpha$ of p_4 Newton's method N_p (see Figure 1(a)) exhibits a fixed point located a $z = \alpha$ (in this case real) while the Secant's method S_p (see Figure 1(b)) has a fixed point at $(x, y) = (\alpha, \alpha) \in \mathbb{R}^2$. We show the two dynamical planes: the complex plane $\mathbb{C}$ for Newton's method and the real plane $\mathbb{R}^2$ for the Secant's method. We plot with the same colour points converging to the same root using both algorithms. However for Newton's method the attracting fixed points are located on the real line $\{z = x + iy \in \mathbb{C} \,|\, y = 0\}$ while for the Secant's method the fixed points are located on the diagonal line $\{y = x\} \subset \mathbb{R}^2$. Similarly Figures 1(c-d) illustrate the same phenomena for $p_5(x) = 5x - 20x^3 + 16x^5$.

We refer to [BF19, GJ19, GJ20], and references therein, for a general background of the Secant's method applied to a polynomial p.

In this paper we emphasize on the behaviour of the Secant's method *near infinity*. As we already noticed, in the Newton's case we might use the complex structure of $\mathbb{S}^2$ to show that via the local chart $\varphi(z) = 1/z$ we have that the Newton's map is conjugated near infinity to

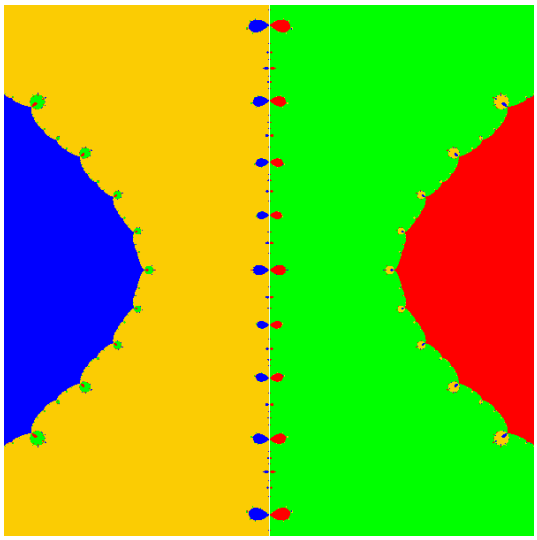

(a) Dynamical plane of the Newton map applied to $p_4(x) = 1 - 8x^2 + 8x^4$.

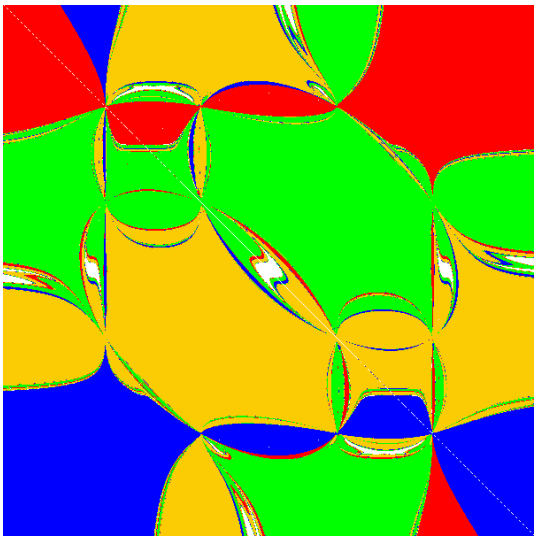

(b) Dynamical plane of the Secant map applied to $p_4(x) = 1 - 8x^2 + 8x^4$.

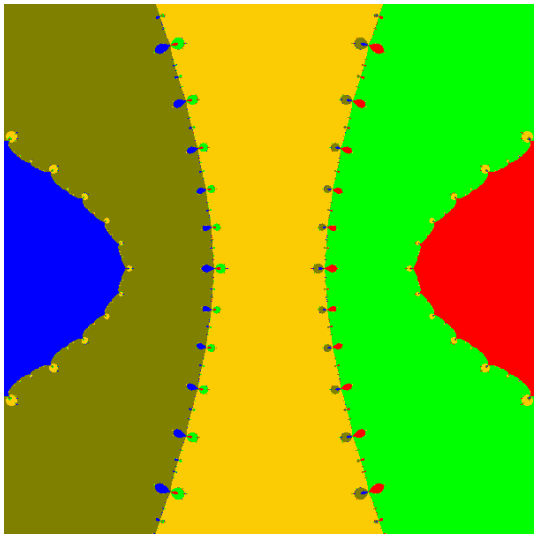

(c) Dynamical plane of the Newton map applied to $p_5(x) = 5x - 20x^3 + 16x^5$.

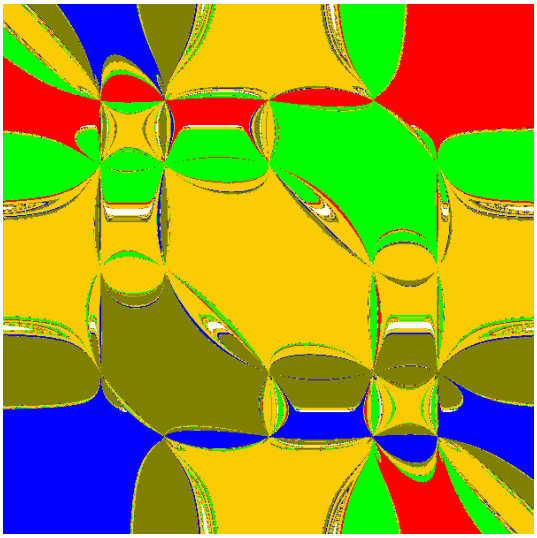

(d) Dynamical plane of the Secant map applied to $p_5(x) = 5x - 20x^3 + 16x^5$.

FIGURE 1. Dynamical planes of the Newton's map (left) and the Secant's map (right) map applied to the Chebychev polynomials $p_4(x) = 1 - 8x^2 + 8x^4$ (top) and $p_5(x) = 5x - 20x^3 + 16x^5$ (bottom). The range of all the pictures is $[-1.5, 1.5] \times [-1.5, 1.5]$.

the map

$$G_p(z) = (\varphi \circ N_p \circ \varphi^{-1})(z) = \frac{1}{N_p(1/z)}$$

near the origin. Thus, Newton's method exhibits a repelling fixed point at $z = \infty$ with multiplier $N_p'(\infty) := G_p'(0) = k/(k-1) > 1$. Moreover it is proven in [HSS01] that $z = \infty$ belongs to the boundary of all immediate basins of attraction of all fixed points of N_p, or equivalently, the immediate basins of attraction of all fixed points (roots of p) of N_p are unbounded. This crucial property is used in [HSS01] to determine a universal set of initial conditions, only depending on k (the degree of p), from which we can find all roots of p at once.

Our goal is to *extend* the Secant's map *to infinity* and see the potential consequences and numerical applications. In this case, however, we cannot add just a point as we did with the Newton case. Instead we use the compactification of $\mathbb{R}^2$ given by the projective plane $\mathbb{RP}^2$. A first step is to extend S, using homogeneous coordinates, to a map $\hat{S}$ on $\mathbb{RP}^2$. Once this is done we observe that $\hat{S}$ itself induce a map $\hat{S}_\infty$ over the line at infinity of $\mathbb{RP}^2$. The expression of $\hat{S}_\infty$ only depends on the degree k of the polynomial p. In Lemma 3.2 we study the dynamics of $\hat{S}_\infty$ and we show that, qualitatively, it only depends on the parity of k.

Alternatively, the map $\hat{S}_\infty$ at a given point on the line at infinity can also be defined as the limit behaviour of S over a line *ending* at this point-direction. This is well defined at all point-directions except the horizontal one since

$$\lim_{x\to\infty} S_p(x, y_0) = (y_0, y_0), \tag{4}$$

and so $\hat{S}([1:0:0])$ would be a point in $\mathbb{R}^2$.

In Figure 2 we show the dynamical plane of the Newton's method and the Secant's method applied to the Chebyshev polynomials $p_4(x) = 1 - 8x^2 + 8x^4$ and $p_5(x) = 5x - 20x^3 + 16x^5$, but now we focus our attention on the behaviour of S near infinity (compare with Figure 1). To do so, we show the dynamical planes inside a large circle centerer at the origin. In Figures 2(a) and (c) we can see that the immediate basins of attraction of the roots of p approach infinity forming wide accesses or sectors and this was the basic idea behind the mentioned results in [HSS01] to determine a universal set of initial conditions. In contrast, the Secant's method near infinity seems to be only related with the largest (red) and smallest (blue) roots of p with the exception of two (k odd) or three (k even) points. The reason for this to happen is a direct consequence Lemma 3.2 and it is explained in Section 5.

Our main result is the study of the global dynamics of $\hat{S}_\infty$. That is, to show that S defines a map over the line at infinity of $\mathbb{RP}^2$ and that such dynamics only depends on k, the degree of the polynomial p. Let $k \geq 3$ and let $\varphi_k : \mathbb{R} \to \mathbb{R}$ be the real map defined by

$$\varphi_k(\zeta) = \frac{\zeta^{k-1} - 1}{\zeta^k - 1} = \frac{\zeta^{k-2} + \zeta^{k-3} + \ldots + \zeta + 1}{\zeta^{k-1} + \zeta^{k-2} + \ldots + \zeta + 1}. \tag{5}$$

Theorem A. *Let p be a degree k polynomial and*

$$\Delta = \bigcup_{n=0}^{\infty} \varphi_k^{-n}(-1). \tag{6}$$

Then, the following statements hold.

(a) *If k is odd, then there exists a unique fixed point $[1:\eta_k:0]$ in ℓ_∞ for $\hat{S}_\infty$, which is attracting. Moreover, $\hat{S}_\infty^n([1:\zeta:0]) \to [1:\eta_k:0]$ as $n \to \infty$, for all $\zeta \in \mathbb{R} \setminus \{0, -1\}$.*

(b) *If k is even, then $\hat{S}_\infty$ has exactly two fixed points: one attracting $[1:\eta_k:0]$ and one repelling $[1:\tau_k:0]$. Furthermore, we have that $\hat{S}_\infty^n([1:\zeta:0]) \to [1:\eta_k;0]$ as $n \to \infty$, for all $\zeta \neq \{0\} \cup \{\tau_k\} \cup \Delta$.*

The paper is organized as follows. In Section 2 we introduce homogeneous coordinates to define $\hat{S}$ in $\mathbb{RP}^2$. In section 3 we prove Theorem A. In section 4 we extend $\hat{S}$ in $\mathbb{CP}^2$ and study the global dynamics of this extension at infinity. In Section 5 we conclude some numerical considerations.

We would like to thank the anonymous referees of a previous version of this paper. We learn from their reports a better way to approach our results.

2. The secant map on $\mathbb{RP}^2$

In this section we extend the Secant map S to the *infinity* by considering its expression over the whole the projective plane $\mathbb{RP}^2 = \mathbb{R}^2 \sqcup \mathbb{RP}^1$, where $\sqcup$ denotes a disjoint union. In this way the *line at infinity* is represented by $\mathbb{RP}^1$ or ℓ_∞. In the complex version we use the notation $\mathbb{CP}^2 = \mathbb{C}^2 \sqcup \mathbb{CP}^1$ instead of $\mathbb{RP}^2$ and in this case the line at infinity is the Riemann sphere.

Recall that $\mathbb{RP}^2$ is a compact, non orientable space which can be associated to the set of lines through the origin in $\mathbb{R}^3$. On the one hand we identify every line through the origin not contained in the plane $z = 0$ with the intersection point between this line and the plane $z = 1$. So, we might parametrize these points by $\left[x : y : 1\right]$ (this is precisely $\mathbb{R}^2$ in the definition of $\mathbb{RP}^2$ above). See Figure 3(a).

The set of lines excluded in this construction, that is the lines contained in $z = 0$, form the so called *line at infinity* of the real projective plane. The coordinate $\left[0 : \zeta : 0\right]$ of a point in ℓ_∞ is determine by the slope of the line $\zeta := y/x$ when $x \neq 0$ and the remaining point directly by $\left[0 : 1 : 0\right]$. See Figure 3(b). Notice that antipodal points are identified. All together determine the coordinate of each point in $\mathbb{RP}^2$, also called *homogeneous cordinates*

$$\mathbb{RP}^2 = \mathbb{R}^2 \sqcup \mathbb{RP}^1 = \begin{cases} \left[x : y : 1\right] & \text{with } (x, y) \in \mathbb{R}^2 \\ \left[1 : \zeta : 0\right] & \text{with } \zeta \in \mathbb{R} \\ \left[0 : 1 : 0\right] \end{cases} \tag{7}$$

If $[x : y : z]$ are the homogenous coordinates in $\mathbb{RP}^2$, the expression of the Secant map in (3) writes, in the $z = 1$ coordinate chart (that is, $(x, y) \leftrightarrow [x : y : 1]$), as a rational map $\hat{S}$ given by

$$\begin{aligned} \hat{S}[x : y : z] = \hat{S}[x/z : y/z : 1] &= \left[y/z : \frac{y/z\ p\,(x/z) - x/z\ p\,(y/z)}{p\,(x/z) - p\,(y/z)} : 1 \right] \\ &= \left[y\,(p\,(x/z) - p\,(y/z)) : y\ p\,(x/z) - x\ p\,(y/z) : z\,(p\,(x/z) - p\,(y/z)) \right]. \end{aligned} \tag{8}$$

So, denoting by

$$q(t, z) = z^k p(t/z) = a_k t^k + a_{k-1} t^{k-1} z + \ldots + a_0 z^k$$

direct computations from (8) give the following expression of $\hat{S}$ as a 3-tuple of homogeneous polynomials

$$\begin{aligned} \hat{S}[x : y : z] &= \left[y\,(p\,(x/z) - p\,(y/z)) : y\ p\,(x/z) - x\ p\,(y/z) : z\,(p\,(x/z) - p\,(y/z)) \right] \\ &= z^k \left[y\,(p\,(x/z) - p\,(y/z)) : y\ p\,(x/z) - x\ p\,(y/z) : z\,(p\,(x/z) - p\,(y/z)) \right] \\ &= \left[y\,(q\,(x, z) - q\,(y, z)) : y\ q\,(x, z) - x\ q\,(y, z) : z\,(q\,(x, z) - q\,(y, z)) \right] \\ &= \left[y(x^k - y^k) + O(z) : \left(yx^k - xy^k \right) + O(z) : O(z) \right] \end{aligned} \tag{9}$$

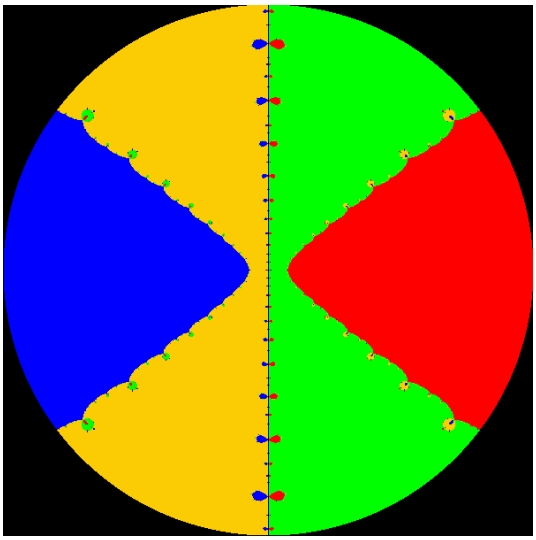

(a) Dynamical plane of the Newton map applied to $T_4(x) = 1 - 8x^2 + 8x^4$.

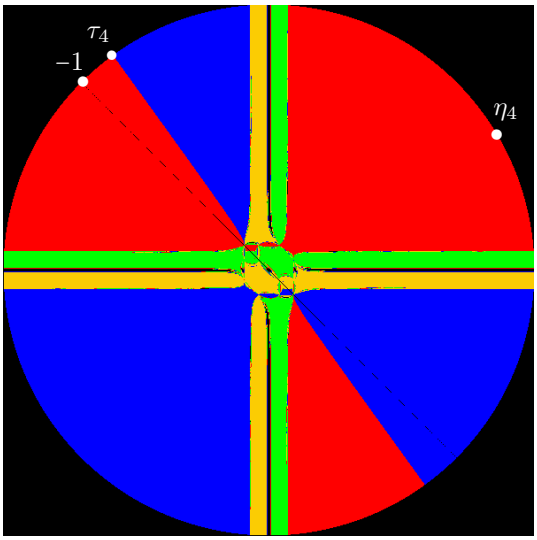

(b) Dynamical plane of the Secant map applied to $T_4(x) = 1 - 8x^2 + 8x^4$.

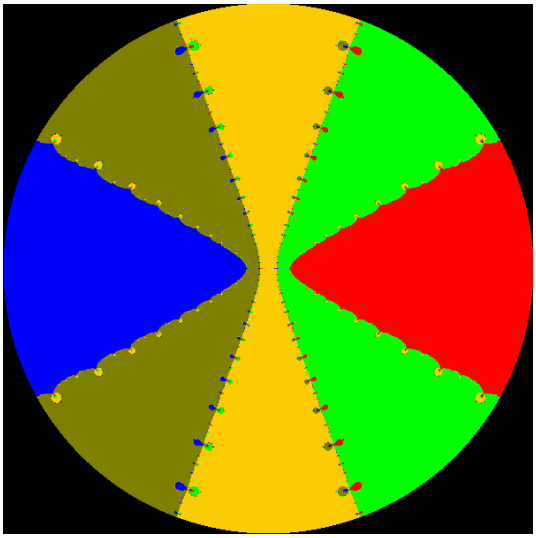

(c) Dynamical plane of the Newton map applied to $T_5(x) = 5x - 20x^3 + 16x^5$.

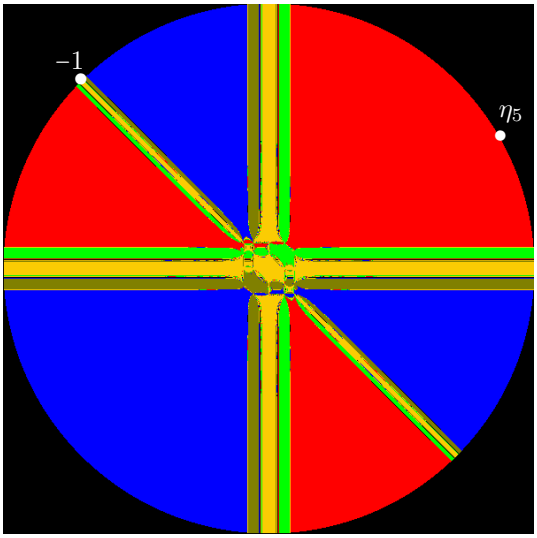

(d) Dynamical plane of the Secant map applied to $T_5(x) = 5x - 20x^3 + 16x^5$.

FIGURE 2. Dynamical planes of the Newton (left) and Secant (right) map applied to the Chebychev polynomials $T_4(x) = 1 - 8x^2 + 8x^4$ (top) and $T_5(x) = 5x - 20x^3 + 16x^5$ (bottom). We show the dynamical plane inside the disk centered at the origin with radius 10, points outside this disk are colored in black.

Remark 1. *The indeterminacy points of* $\hat{S}$ *are given by 3-tuples* $[x : y : z]$ *such that* $\hat{S}[x : y : z] = [0 : 0 : 0]$. *According to* (9) *we have*

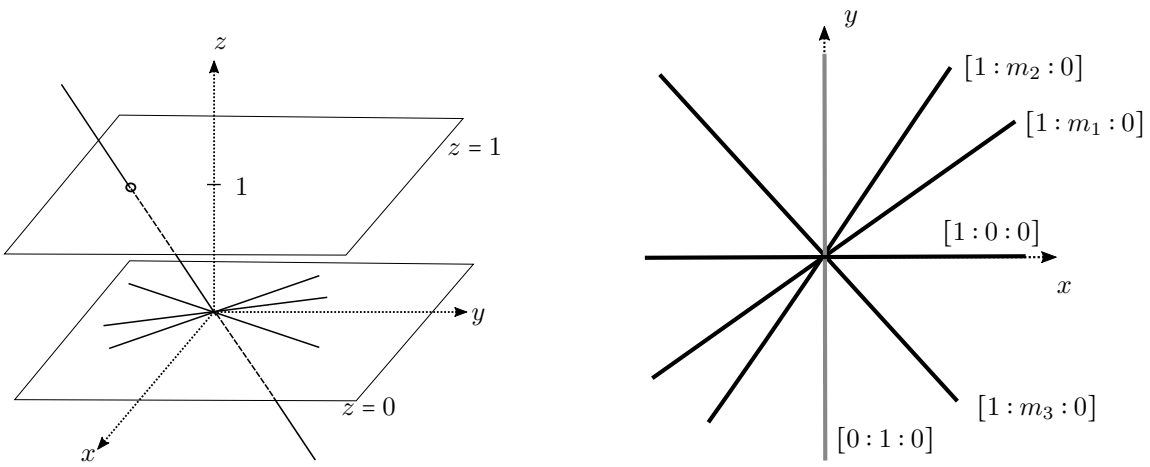

(a) The space of all lines through the origin in $\mathbb{R}^3$ not contained in the plane $z = 0$.

(b) The space of all lines through the origin in the plane $z = 0$.

FIGURE 3. A model for the real projective plane $\mathbb{RP}^2 = \mathbb{R}^2 \sqcup \ell_\infty$ (a). The line of infinity ℓ_∞ (b).

(a) *Finite indeterminacy points ($z = 1$ in homogeneous coordinates). They correspond to points (x, y) such that $x \neq y$ and $p(x) = p(y) = 0$. For a discussion of finite indeterminacy points we refer to* [GJ19] *where they are called focal points.*
(b) *Points at infinity ($z = 0$ in homogeneous coordinates) such that $y = 0$ and $x \neq 0$, or $x = y$ and $xy \neq 0$ (that is, $\{[1 : 0 : 0], [1 : 1 : 0]\}$, see the last expression in (9)).*

3. Proof of Theorem A

We split the proof of Theorem A in two technical lemmas. First we observe that $\hat{S}$ defines a map over the line at infinity.

Lemma 3.1. *Consider a polynomial p as defined in (2). Denote $\zeta = y/x$ and assume generically that $xy \neq 0$. Then the Secant map S induces a map $\hat{S}_\infty : \ell_\infty \to \ell_\infty$ given by*

$$\hat{S}_\infty[1 : \zeta : 0] = [1 : \varphi_k(\zeta) : 0]. \tag{10}$$

Moreover the points $\{[1 : 0 : 0], [1 : 1 : 0]\}$ are indeterminacy points of the secant map at infinity.

Proof. The restriction of the Secant map (9) at infinity, that is with $\{z = 0\}$, under the generic condition $xy \neq 0$, writes as

$$\hat{S}_\infty[x : y : 0] = \left[x^k - y^k : \left(x^k - xy^{k-1}\right) : 0\right] = \left[1 : \frac{x\left(x^{k-1} - y^{k-1}\right)}{(x^k - y^k)} : 0\right].$$

If $\zeta = y/x$ and we consider φ_k as defined in (5), we immediately conclude (10). The indeterminacy points at infinity follows from the previous remark. □

From the previous lemma it follows that the dynamics of $\hat{S}_\infty$ is governed by the dynamics of the map φ_k in $\mathbb{R}$.

Lemma 3.2. *The following statements hold.*

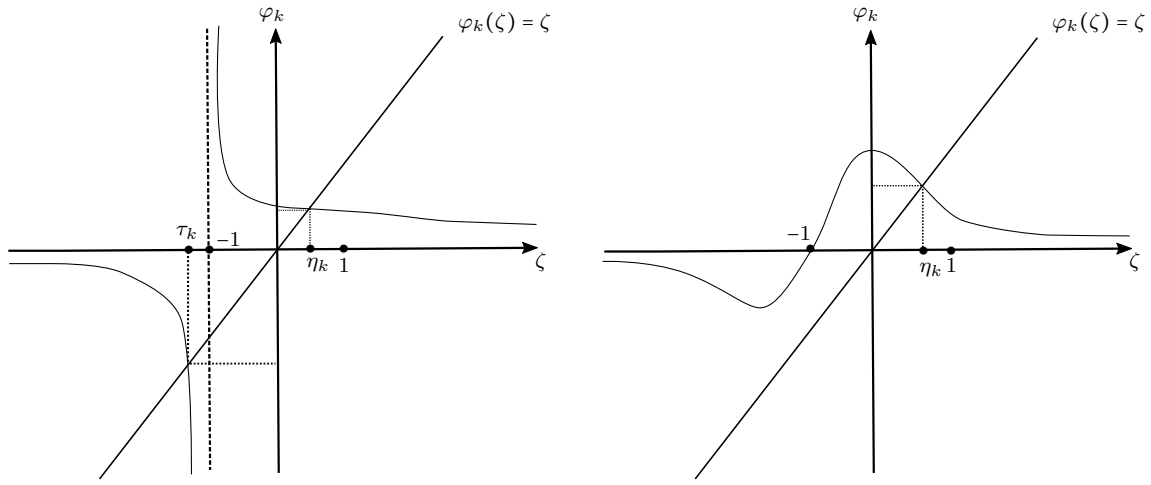

(a) Graphic of φ_k for k even.

(b) Graphic of φ_k for k odd.

FIGURE 4. The qualitative graph of the auxiliary map φ_k in $\mathbb{R}$ depending on the parity of k.

(a) *If k is odd, the map φ_k has a unique fixed point η_k. Moreover, $\eta_k \in (0,1)$ and it is a global attractor, i.e., $\varphi_k^n(\zeta) \to \eta_k$ as $n \to \infty$ for all $\zeta \in \mathbb{R}$.*

(b) *If k is even, the map φ_k has exactly two fixed points. One, $\eta_k \in (0,1)$, is attracting. The other $\tau_k < -1$ is repelling. Moreover, $\varphi_k^n(\zeta) \to \eta_k$ as $n \to \infty$ for all $\zeta \in \mathbb{R} \setminus \Delta \cup \{\tau_k\}$, where Δ is defined in* (6).

Proof. We first prove (b). Clearly the map $\varphi_k(\zeta)$ has a unique vertical asymptote at $\zeta = -1$, and a horizontal asymptote at $y = 0$ since $\varphi_k(\zeta) \to 0^{\pm}$ as $\zeta \to \pm\infty$. Easy computations show

$$\varphi_k'(\zeta) = -\frac{\zeta^{k-2}}{(x^k-1)^2}\psi_k(\zeta), \tag{11}$$

where $\psi_k(\zeta) = \left(\zeta^k - [k(\zeta-1)+1]\right)$. We have that $\operatorname{sign}\left(\varphi_k'(\zeta)\right) = -\operatorname{sign}\left(\psi_k(\zeta)\right)$ since k is an even number. But observe that $\psi_k(\zeta)$ measures the difference from the graph of the function $y = \zeta^k$ and the graph of the function $y = k(\zeta-1)+1$ which is precisely the tangent line to the graph of $y = \zeta^k$ at the point $\zeta = 1$. Hence $\psi_k(\zeta) \geq 0$ for all $\zeta \in \mathbb{R}$ and $\psi_k(\zeta) = 0$ if and only if $\zeta = 1$. In particular this implies that φ_k is strictly decreasing in its domain of definition. All together prove that φ_k has exactly two fixed points: $\tau_k < -1$ and $\eta_k \in (1/2, 1)$ (notice that $\varphi_k(1/2) > 1/2$ and $\varphi_k(1) = (k-1)/k < 1$). See Figure 5(b).

We claim that the positive fixed point η_k is attracting by showing that $|\varphi_k'(\eta_k)| < 1$, and the negative fixed point τ_k is repelling by showing that $|\varphi_k'(\tau_k)| > 1$. We consider each case in turn. To see this we notice that $\varphi_k'(\zeta)$ writes as

$$\varphi_k'(\zeta) = -\frac{\zeta^{k-2}\left(\zeta^{k-2} + 2\zeta^{k-3} + \ldots + (k-2)\zeta + k - 1\right)}{\left(\zeta^{k-1} + x^{k-2} + \ldots + \zeta + 1\right)^2}.$$

Doing some computations we get

$$\varphi_k'(\zeta) = -\frac{\sum_{j=4}^{k+1}(j-3)\zeta^{2k-j} + (k-1)\zeta^{k-2}}{\psi(\zeta) + \sum_{j=4}^{k+1}(j-1)\zeta^{2k-j} + (k-1)\zeta^{k-2}},$$

where $\psi(\zeta) > 0$ for all $\zeta > 0$ (in fact it is a polynomial with positive coefficients). Accordingly $|\varphi_k'(\zeta)| < 1$ for all $m > 0$ since $j-3 < j-1$ and so the positive fixed point η_k of φ_k is attracting. The rest of the statement of (a) follows easily.

To finish, we prove (b) by showing that $\tau_k < -1$ is repelling since the other statements follow easily. Observe that

$$\varphi_k'(\zeta) = \frac{1}{(\zeta^k-1)^2}\left[(k-1)x^{k-2}\zeta^k - 1) - k\zeta^{k-1}(\zeta^{k-1}-1)\right]$$

and since τ_k is a fixed point of φ_k we conclude that $\tau_k^{k-1} - 1 = \tau_k\left(\tau_k^k - 1\right)$. So some computations give

$$\varphi_k'(\tau_k) = -\frac{\tau_k^{k-2}}{\tau_k^k - 1}\left[k(\tau_k^2 - 1) + 1\right].$$

Since $\tau_k < -1$ and k is even it is clear that $\varphi_k'(\tau_k) < 0$. We claim that $\varphi_k'(\tau_k) < -1$ and so τ_k is a repelling fixed point of φ_k. Indeed

$$-\varphi_k'(\tau_k) > k + \frac{1}{\tau_k^2} - \frac{k}{\tau_k^2} > 1.$$

We secondly assume that k is an odd number. We have that $\varphi_k(\zeta) \to 0^{\pm}$ as $x \to \pm\infty$ but now $\varphi_k(-1) = 0$. See Figure 5 (b). In a similar way as in the even case $\varphi_k(\zeta)$ is a decreasing map for $\zeta \geq 0$ since $\varphi_k'(\zeta) < 0$ for all value of $x \geq 0$. Hence, the map φ_k has a positive fixed point η_k in the interval $(0,1)$ since $\varphi_k(0) = 1$ and $\varphi_k(1) = (k-1)/k$. Using the same arguments as in the even case we conclude that η_k is an attracting fixed point.

Finally, we claim that η_k is the unique fixed point of φ_k when k is an odd number. From (5) have that $\varphi_k(\zeta) = \zeta$ writes as $\zeta^k + \zeta^{k-1} - 1 = 0$ and it is easy to see that the polynomial $q_k(x) = \zeta^k + \zeta^{k-1} - 1$ has a unique real root when k is an odd number, since q_k has a local minimum at 0 with $q_k(0) < 0$ and a local maximum at $-(k-1)/k$ with

$$q_k(-\frac{k-1}{k}) = -\left(\frac{k-1}{k}\right)^k + \left(\frac{k-1}{k}\right)^{k-1} - 1 = \frac{(k-1)^{k-1}}{k^k} - 1 < 0.$$

□

In Table 1 we compute numerically the fixed points of φ_k for several values of k. Combining Lemmas 3.1 and 3.2 we obtain Theorem A.

Proof of Theorem A. The statement of Theorem A is basically a direct consequence of Lemmas 3.1 and 3.2. We only notice that in Theorem A(a) we exclude the point $\zeta = 0$ since in Lemma 3.1 we had assumed $xy \neq 0$, and we exclude $\zeta = -1$ since $\varphi(-1) = 0$. □

4. Further results and the secant map on $\mathbb{CP}^2$

We start this section by studding the the local dynamics of $[1 : \eta_k : 0]$ and $[1 : \tau_k : 0]$ as fixed points of $\hat{S}$ in $\mathbb{RP}^2$ (that is, not only restricted to the line at infinity). We first write

k	attracting fixed point η_k of φ_k	repelling fixed point τ_k of φ_k
2	$\approx$0,61803399	$\approx$-1,61803399
3	$\approx$0,75487766	——
4	$\approx$0,81917251	$\approx$-1,38027757
5	$\approx$0,85667488	——
6	$\approx$0,88127146	$\approx$-1,28519903
7	$\approx$0,89865371	——
8	$\approx$0,91159235	$\approx$-1,23205463
9	$\approx$0,92159932	——
...	...	...
20	$\approx$0.9650705	$\approx$ -1,1186991
...	...	...
50	$\approx$0.9860941	$\approx$ -1.05933705

TABLE 1. Fixed points of the map $\tilde{S}$ on ℓ_∞.

the expression $\hat{S}$ in the $x = 1$ homogeneous coordinate system. We have

$$\begin{aligned}\hat{S}[1:y:z] &= [y\,(q\,(1,z)-q\,(y,z)) : y\;q\,(1,z) - \;q\,(y,z) : z\,(q\,(1,z)-q\,(y,z))]\\ &= \left[1 : \frac{y\;q\,(1,z) - \;q\,(y,z)}{y\,(q\,(1,z)-q\,(y,z))} : \frac{z\,(q\,(1,z)-q\,(y,z))}{y\,(q\,(1,z)-q\,(y,z))}\right]\\ &= \left[1 : \frac{(1-y^{k-1})+O(z)}{(1-y^k)+O(z)} : \frac{z}{y}\right]\end{aligned} \tag{12}$$

Using the notation $(y,z) \leftrightarrow [1:y:z]$ we might rewrite $\hat{S}$ as a map G acting as follows

$$(y,z) \to G(y,z) = \left(\frac{(1-y^{k-1})+O(z)}{(1-y^k)+O(z)}, \frac{z}{y}\right) = (G_1(y,z), G_2(y,z))\,.$$

The differential of G at any point of the form $(\xi,0)$ is a triangular matrix of the form

$$DG(\xi,0) = \begin{pmatrix} \varphi_k'(\xi) & \star \\ 0 & 1/\xi \end{pmatrix} \tag{13}$$

We conclude in the following statement the local behviour of the real fixed points of $\hat{S}$ in ℓ_∞.

Lemma 4.1. *The fixed points $(\eta_k,0)$ and $(\tau_k,0)$ (only for k even), are of saddle type.*

Proof. We know from Lemma 3.2 that, on the one hand, $(\eta_k,0)$ is such that $0 < \eta_k < 1$ and is an attracting fixed point $-1 < \varphi_k'(\eta_k) < 0$, and on the other hand, $(\tau_k,0)$ is such that $\tau_k < -1$ and is a repelling fixed point $\varphi_k'(\tau_k) < -1$. So the lemma follows from (13). □

The previous lemma complete the picture of the local dynamics of the infinite *real* fixed points of $\hat{S}$. However, in $\mathbb{CP}^2$, the equation $\varphi_k(\zeta) = \zeta$ has k solutions, and only one or two of them (depending on the parity of k) have been already studied.

We finish this section by studding the local dynamics around the *non real* infinite fixed points of $\hat{S}$. Clearly (9) and (12) correspond to the expressions of $\hat{S}$ in $\mathbb{CP}^2$, just taking the variables $\{x,y,z\}$ as complex. So, the *infinity* of $\mathbb{CP}^2$ is now a Riemann sphere, $\mathbb{S}^2 = \hat{\mathbb{C}}$, and

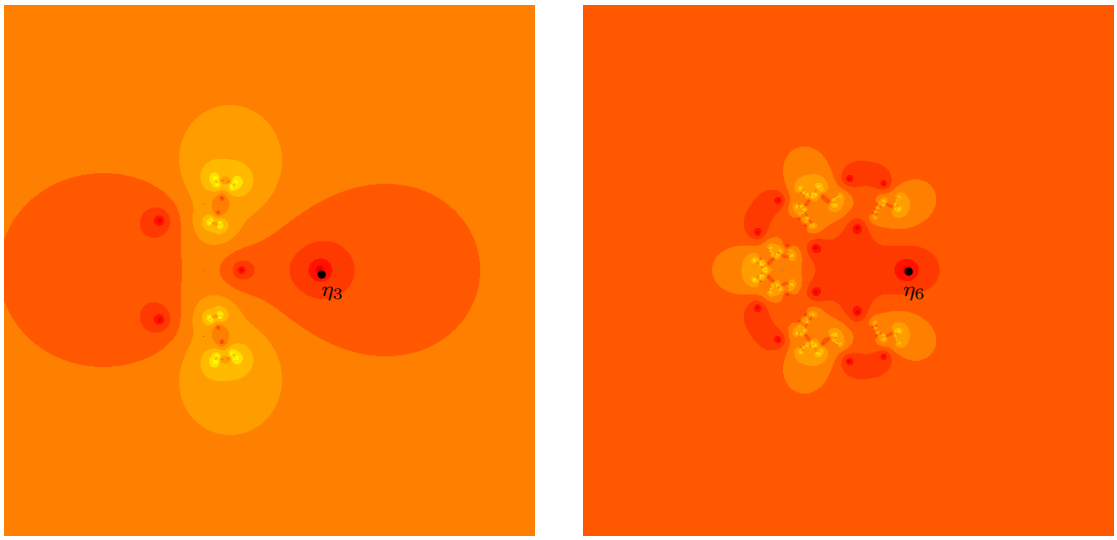

(a) (b)

FIGURE 5. The dynamical planes of φ_k for $k = 3$ (left) and $k = 6$ (right). In orange (gradient orange-to-yellow) we draw the completely invariant immediate basin of attraction of η_k, $k = 3, 6$. The *points* in yellow (intersection of all gradient-orange) correspond to the Julia set which we conjecture it is a Cantor set. So, the Fatou set has a unique component, $\mathcal{A}^\star(\eta_k)$, the immediate basin of attraction of the point η_k, and all fixed points different from η_k are repelling.

the dynamics of $\hat{S}_\infty$ is governed by the complex rational map $\varphi_k : \hat{\mathbb{C}} \to \hat{\mathbb{C}}$ as defined in (5) but now considering $\zeta \in \mathbb{C}$.

Let R be a rational map. We say that a point $z \in \mathcal{F}(R)$, where $\mathcal{F}(R)$ denotes the *Fatou set* of R, if $\{f^n|_U\}_{n\geq 0}$ is a normal family for some sufficiently small enigborhood U of z. In contrast, the *Julia set* is defined as $\mathcal{J}(R) = \hat{\mathbb{C}} \setminus \mathcal{F}(R)$. The Fatou set is open (so, the Julia set is closed) and its connected components are called *Fatou components*. One can easily prove that the immediate basin of the attracting fixed point (as well as its eventual preimages, if any) are Fatou components. See [Mil06] for an excellent reference on complex rational iteration.

In our setting for each $k \geq 3$, the point η_k is an attracting fixed point. We denote by $\mathcal{A}^\star(\eta_k)$ its immediate basin of attraction. We conjecture that all critical points belong to $\mathcal{A}^\star(\eta_k)$ and then by Theorem 9.8.1 in [Bea91] the Julia set of φ_k is a Cantor set. Consequently all periodic points (of any period) different from η_k are repelling. In what follows we assume that all fixed points different from η_k are repelling as fixed points of $\hat{S}_\infty$ in $\hat{\mathbb{C}}$.

To study their local character as fixed points of $\hat{S}$ in $\mathbb{CP}^2$, according to (13), we need to know if their modulus is greater or smaller than 1. A direct computation shows that for $k = 3$ the two fixed points different from η_3 has modulus bigger than 1 (and so they are repelling fixed points in $\mathbb{CP}^2$) while for $k \geq 4$ there are fixed points of modulus greater and smaller than 1, and hence for $k \geq 4$ the fixed points can be saddle or repelling fixed points.

5. Conclusions

Theorem A describes the dynamics of $\hat{S}_\infty$ as a map of $\ell_\infty \subset \mathbb{RP}^2$, and it points out some differences depending on the parity of k (we illustrate these behaviours in Figures 2(b) and (d)).

The first consideration is that $\hat{S}_\infty$ always has an attracting fixed point $[1:\eta_k:0]$ which basically trapped all the dynamics on the line at infinity; that is, except for a countable discrete set of points on ℓ_∞, all initial conditions converge to $[1:\eta_k:0]$. It is worth to notice that this fixed point has a direct link with the two external roots of p; the largest and the smallest root of p which have wide sectors inside the immediate basin with $[1:\eta_k:0]$ on their (infinite) boundaries. Notice also that diametrical opposite points in the circle correspond to the same homogenous coordinate.

Secondly, we proved that the dynamics of $\hat{S}_\infty$ is governed by the dynamics of the real map φ_k. We restrict now to k even (see Figure 5(a)). Clearly $x=-1$ is a vertical asymptote and $y=0$ is an horizontal asymptote. In Lemma 3.2 we proved that φ_k has one attractive fixed point η_k, and one repelling fixed point $\tau_k<-1$. Except for the preimages of $x=-1$ and the point $x=\tau_k$ any other point tends to τ_k under iteration. How this translates to the dynamics of $\hat{S}_\infty$? Outside the points $[1:0:0]$, $[0:1:0]$ and $[1:-1:0]$ the map $\hat{S}_p$ reflects trivially the dynamics of φ_k, so every orbit converge to $[1:\eta_k:0]$. In fact $[1:0:0]$ is the *endpoint* the horizontal lines $L_j=\{(x,\alpha_j),\ x\in\mathbb{R},\ j=0,\dots n\}$ and it is an exercise to prove that, at least for large values of x, $L_j\in A(\alpha_j)$. This explains why we *see* in Figure 2(b) all *colours* (corresponding to all roots of p) landing at this point in ℓ_∞. Now, since $y=0$ is an horizontal asymptote for φ_k and $\hat{S}_p([0:1:0])=[1:0:0]$ we see *a copy* of the previous structure in the vertical direction. Thus, it only remains to discuss the point $[1:-1:0]$. Certainly $\hat{S}_p$ has a pole at this point since $\varphi(-1)=\infty$ but it is possible to *redefine* $\hat{S}[1:-1:0]:=[1:1:0]$ (we just use that

$$\lim_{x\to\infty} S(x,-x)=[1:1:0]$$

and this is the reason why in Figure 2(b) we see *nothing* but red in a neighbourhood of $[1:-1:0]$.

If k is odd (see Figure 5(b) and Figure 2(d)), since

$$\lim_{x\to\pm\infty}\varphi_k(x)=0 \quad\text{and}\quad \varphi_k(-1)=0$$

the point $[1:0:0]$ has two preimages: $[0:1:0]$ and $[1:-1:0]$. So, using the same arguments as above, we see all colours landing at $[1:0:0]$ and in each of the two preimages. Since

$$\varphi_k^n(x)=\eta_k,\ x\neq\mathbb{R}\setminus\{-1\}$$

we easily conclude that $\hat{S}^n([1:x:0])\to[1:\eta_k:0]$ as $n\to\infty$, for all $x\in\mathbb{R}\setminus\{0,-1\}$.

References

[Bea91] Alan F. Beardon. *Iteration of rational functions*, volume 132 of *Graduate Texts in Mathematics*. Springer-Verlag, New York, NY, 1991.

[BF19] Eric Bedford and Paul Frigge. The secant method for root finding, viewed as a dynamical system. *Dolomites Research Notes on Approximation, to appear*, 2019.

[BFJK14] Krzysztof Barański, Núria Fagella, Xavier Jarque, and Bogusława Karpińska. On the connectivity of the Julia sets of meromorphic functions. *Invent. Math.*, 198(3):591–636, 2014.

[BFJK18] Krzysztof Barański, Núria Fagella, Xavier Jarque, and Bogusł awa Karpińska. Connectivity of Julia sets of Newton maps: a unified approach. *Rev. Mat. Iberoam.*, 34(3):1211–1228, 2018.

[Cay79a] Arthur Cayley. Applications of the Newton-Fourier Method to an imaginary root of an equation. *Quat. J. of Pure and App. Math.*, 16:179–185, 1879.

[Cay79b] Arthur Cayley. The Newton-Fourier Method imaginary problem. *Am. J. of Math.*, 2:97, 1879.

[Cay80] Arthur Cayley. On the Newton-Fourier imaginary problem. *Proc. Camb. Phil. Soc.*, 3:231–232, 1880.

[GJ19] Antonio Garijo and Xavier Jarque. Global dynamics of the real secant method. *Nonlinearity*, 32(11):4557–4578, 2019.

[GJ20] Antonio Garijo and Xavier Jarque. The secant map applied to a real polynomial with multiple roots. To appear in Discrete and Continuous Dynamical Systems, 2020.

[HSS01] John Hubbard, Dierk Schleicher, and Scott Sutherland. How to find all roots of complex polynomials by Newton's method. *Invent. Math.*, 146(1):1–33, 2001.

[Mil06] John Milnor. *Dynamics in one complex variable*, volume 160 of *Annals of Mathematics Studies*. Princeton University Press, Princeton, NJ, third edition, 2006.

[Shi09] Mitsuhiro Shishikura. The connectivity of the Julia set and fixed points. In *Complex dynamics*, pages 257–276. A K Peters, Wellesley, MA, 2009.

Departament d'Enginyeria Informàtica i Matemàtiques, Universitat Rovira i Virgili, 43007 Tarragona, Catalonia.

Email address: antonio.garijo@urv.cat

Departament de Matemàtiques i Informàtica at Universitat de Barelona and Barcelona Graduate School of Mathematics, 08007 Barcelona, Catalonia.

Email address: xavier.jarque@ub.edu